Nickel–heterocumulene complexes stabilized by trimethylphosphine: Synthesis, characterization and catalytic application in organozinc coupling with CS_2

Ning Huang, Xiaoyan Li, Wengang Xu, Hongjian Sun *

School of Chemistry and Chemical Engineering, Shandong University, Shanda Nanlu 27, 250100 Jinan, PR China

ARTICLE INFO

ABSTRACT

The reactivity of $Ni(PMe_3)_4$ with CO_2, CS_2 and SCNPh was studied. Although CO_2 is structurally homologous compound with CS_2 and SCNPh, its reactivity with $Ni(PMe_3)_4$ shows a different result with those of CS_2 and SCNPh. Reactions of $Ni(PMe_3)_4$ with carbon disulfide and phenyl isothiocyanate in THF give the tetrahedral coordinate complexes $(Me_3P)_3Ni(\eta^2\text{-}CS_2)$ (**1**) and $(Me_3P)_3Ni(\eta^2\text{-}SCNPh)$ (**3**), characterized by standard spectroscopic methods and X-ray diffraction. Nickel(0) complexes **1** and **3** are stabilized by the strong donor ligand PMe_3. In the case of CO_2, attempts to isolate the expected nickel(0) complex $(Me_3P)_3Ni(\eta^2\text{-}CO_2)$ (**4**) proved to be unsuccessful. To further extend the utility of our nickel catalysts, the catalytic coupling of organozinc bearing different functionalities with CS_2 was explored. With 10 mol% of **1** as the catalyst, MeZnMe, EtZnEt and PhZnBr coupled with CS_2 to form the corresponding methyl dithiocarboxylate following esterfication of the initial products.

© 2012 Elsevier B.V. All rights reserved.

1. Introduction

The reactivity of heterocumulenes such as carbon dioxide and carbon disulfide, which are promising sources of C1 chemistry, with transition metal complexes has been reviewed [1–3] and has been shown to produce a variety of chemical transformations [4–7]. The development of practical methods for the generation of organic compounds from carbon dioxide, an abundant and inexpensive source of carbon, is essential in the future management of this greenhouse gas. Carbon disulfide and phenyl isothiocyanate are highly reactive, and their coordination, addition, cleavage, and insertion reactions are currently being intensively investigated. The interest in the coordination chemistry of carbon disulfide and phenyl isothiocyanate with transition metal complexes stems mainly from the fact that both of them are structurally related to carbon dioxide [8–11] although it is clear that these molecules exhibit different reactivity.
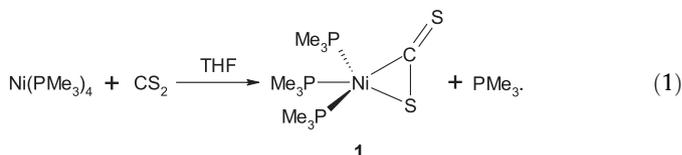
Since Aresta isolated the first CO_2 adduct $(PCy_3)_2Ni(\eta^2\text{-}CO_2)$ [12–14], several examples of late transition-metal carbon dioxide coordination compounds have been reported with various binding modes [12–15]. Carbon dioxide complexes of nickel have been extensively studied due to their involvement in catalytic transformations [16]. As part of our studies on the coordination chemistry of $Ni(PMe_3)_4$, we are interested in the reactivity of CO_2 with $Ni(PMe_3)_4$ and seek to investigate the binding of nickel(0) with CO_2 and its congeners, CS_2 and SCNPh. Herein, we report our initial

studies on the reactivity of $Ni(PMe_3)_4$ with CO_2, CS_2 and SCNPh under mild conditions.

2. Results and discussion

2.1. Reaction of $Ni(PMe_3)_4$ with CS_2

When a solution of CS_2 in THF was treated with $Ni(PMe_3)_4$ in diethyl ether, the mixture turned from light yellow to dark red immediately and compound **1** was isolated as a red solid in the yield of 81% upon workup, which could be crystallized from diethyl ether at 0 °C (Eq. (1)). The ^1H NMR spectrum of **1** displays only one set of methyl groups at room temperature.

$$Ni(PMe_3)_4 + CS_2 \xrightarrow{THF} \underset{\textbf{1}}{\left[\begin{array}{c} Me_3P \\ Me_3P \end{array}\!\!\!\!Ni\!\!\!\overset{S}{\underset{S}{\diagdown}}\!\!C\!\!=\!\!S\right]} + PMe_3. \quad (1)$$

Crystals of **1** suitable for X-ray diffraction were grown from a diethyl ether solution at −20 °C. The molecular structure of one of two independent molecules in the unit cell of **1** is shown in Fig. 1 and indicates a tetrahedral coordination geometry at nickel with the π-coordinate C=S at one vertex of the tetrahedron. **1** is stable in air for several hours. X-ray crystallography confirmed the molecular configuration of **1** derived from solution data. The length of uncoordinated C–S bond is at 1.634(3) Å, while the η^2-coordinated C1–S1 bond length is at 1.647(3) Å. The coordination of C–S bond makes it a little bit longer.
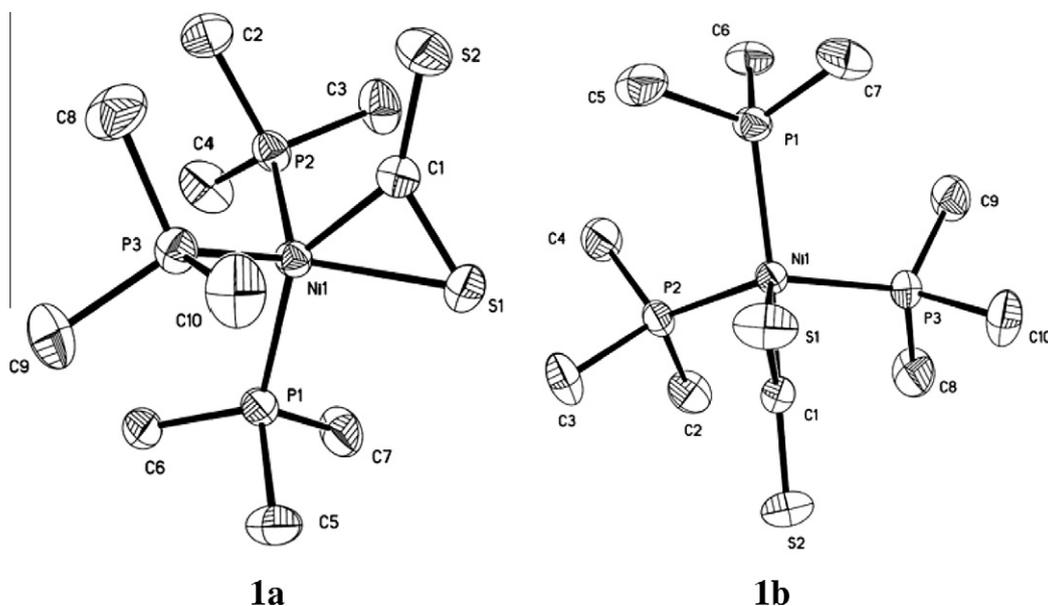
1a

1b

Fig. 1. Perspective views of the structure of **1** with H atoms omitted for clarity and thermal ellipsoids drawn at 50% probability. (**1a**) Side view of the skeleton of $(PMe_3)_3Ni(\eta^2\text{-}CS_2)$. (**1b**) Top view of the same skeleton.

Complex **1** presents a constant primary geometry where a metal fragment of L_3M type, formed by the metal and three phosphorus atoms, is η^2-bonded to a C–S linkage of the heteroallene (CS_2). Selected bond distances and angles for compounds **1** and **3** are reported in Table 1.

Other tetra-coordinate CS_2-nickel complexes were previously disclosed [17,18]. Nevertheless, no crystallographic data for them were provided. In the IR spectra (Nujol mull) of complex **1** the vibrations at 1149 and 638 cm^{-1} can be assigned to the C=S and C–S bonds, respectively. They are very close to 1145 ($\nu_{C=S}$) and 639 (ν_{C-S}) cm^{-1} reported for (dtbpe)Ni(η^2-CS_2) by Hillhouse [19].

2.2. Reaction of 1 with iodomethane
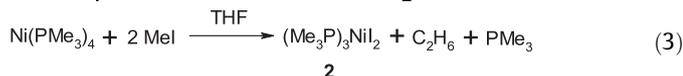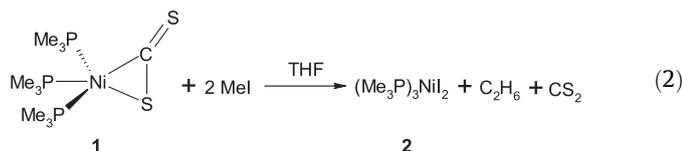
Motivated by our results of nickel from Eq. (1), we investigated the reaction of iodomethane with **1**. **1** reacted with excess iodomethane in THF by dissociation, undergoing an intermolecular

oxidative addition reaction (Eq. (2)) to afford $(Me_3P)_3NiI_2$ with the escape of ethane. This reaction has no distinct difference with the one of Ni(PMe$_3$)$_4$ and MeI (Eq. (3)) [20], which indicates that the CS_2 adduct $(PMe_3)_3Ni(\eta^2\text{-}CS_2)$ (**1**) shows a similar reactivity with Ni(PMe$_3$)$_4$ in this case.

2.3. Reaction of Ni(PMe₃)₄ with SCNPh
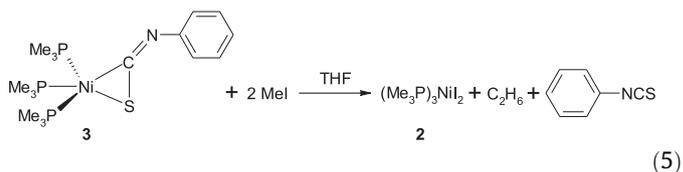
Treating a diethyl ether solution of phenyl isothiocyanate with Ni(PMe$_3$)$_4$ gave rise to η^2-(C,S) nickel complex **3** (Eq. (4)). Crystallization at -20 °C afforded a red crystalline solid in 72% isolated yield. Complex **3** both in the solid state and in solution is stable (without the change of habitus and color) at room temperature in the air for 10 min at least.
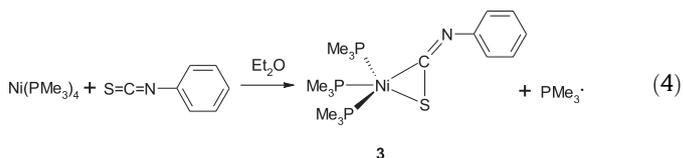
Similar to the formation of nickel complex **1**, the isothiocyanate group is also in η^2-(C,S) bonding mode in complex **3**, which was largely accepted in the literature [21,22], but the structural evidence for this is seldom [23–26], as is shown in Fig. 2. The IR spectrum (Nujol Mull) exhibits a band at 1607 cm^{-1} for the C=N stretching vibration, while the normal value for PhNCS is 1645 cm^{-1}. The rather low value for the C=N frequency is due to significant electron transfer to the –NCS unit from the nickel atom. This nickel atom is very electron rich because trimethylphosphine is a strong donor ligand.

2.4. Reaction of 3 with iodomethane

$$\text{(2)}$$

$$Ni(PMe_3)_4 + 2\,MeI \xrightarrow{\text{THF}} \underset{\mathbf{2}}{(Me_3P)_3NiI_2} + C_2H_6 + PMe_3 \quad (3)$$

$$\text{(4)}$$

Table 1
Selected bond distances (Å) and angles (°) for **1** and 3.

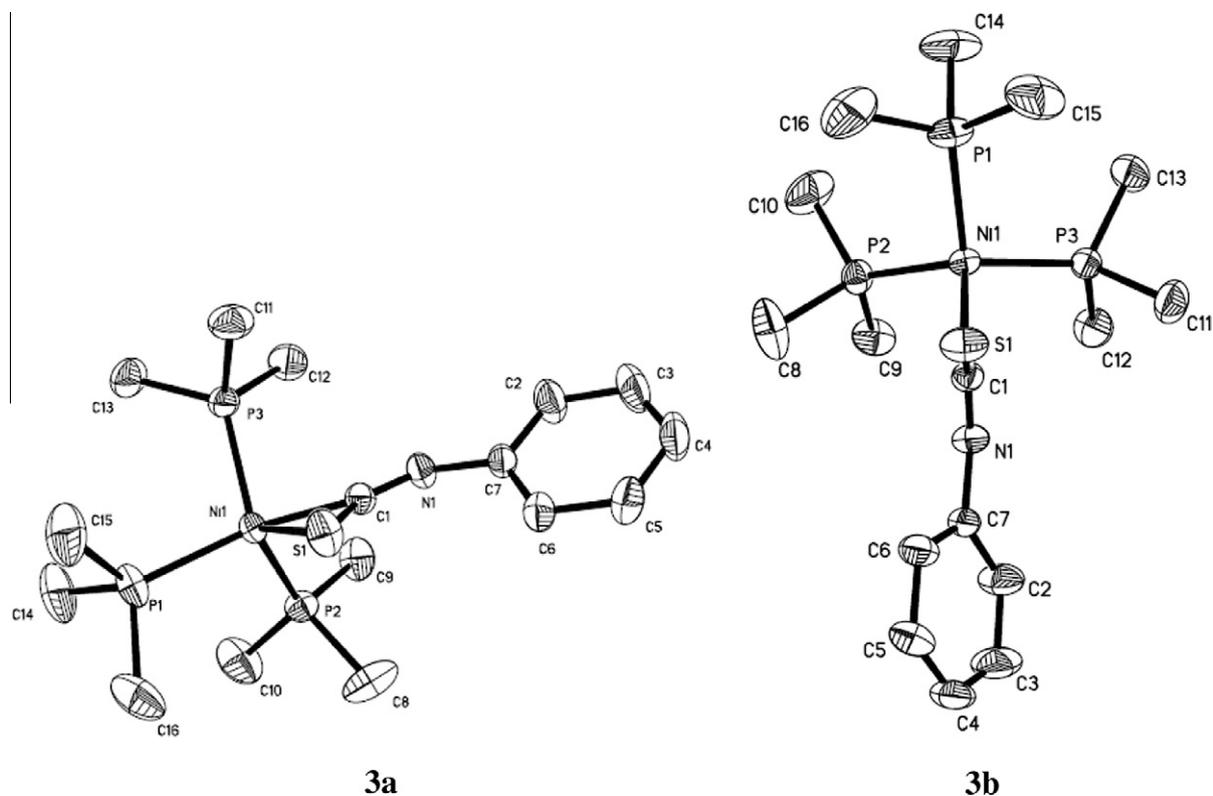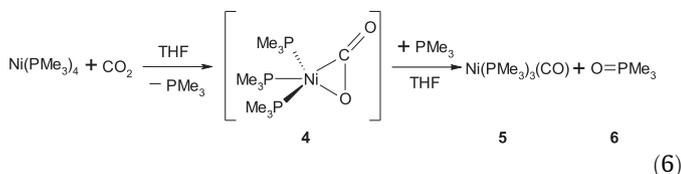| Complex **1**			
Ni1–S1	2.2786(11)	Ni1–P1	2.2183(10)
Ni1–C1	1.856(3)	C1–S1	1.647(3)
C1–S2	1.634(3)	C2–P2	1.826(3)
S1–C1–Ni1	80.90(14)	S2–C1–Ni1	142.1(2)
S2–C1–S1	136.9(2)	C1–Ni1–S1	45.54(10)
P1–Ni1–S1	99.56(4)	C1–S1–Ni1	53.56(11)
C1–Ni1–P3	94.48(10)		
Complex **3**			
Ni1–S1	2.3054(7)	Ni1–C1	1.8675(19)
Ni1–P1	2.1886(8)	C1–S1	1.707(2)
N1–C1	1.254(3)		
C1–Ni1–P1	148.25(6)	C1–Ni1–S1	46.85(6)
P1–Ni1–S1	101.57(2)	C1–S1–Ni1	52.96(6)
N1–C1–S1	142.23(16)	N1–C1–Ni1	137.58(16)

$$\text{(5)}$$

Fig. 2. Perspective views of the structure of **3** with H atoms omitted for clarity and thermal ellipsoids drawn at 50% probability. (**3a**) Side view of the skeleton of $(PMe_3)_3Ni(\eta^2\text{-}SCNPh)$. (**3b**) Top view of the same skeleton.

The reaction of nickel complex **3** with excess iodomethane in THF resulted in intermolecular oxidative addition to diiodo nickel(II) complex **2** with the escape of ethane (Eq. (5)). The coordinated phenyl isothiocyanate was released.

2.5. Reaction of Ni(PMe₃)₄ with CO₂

$$Ni(PMe_3)_4 + CO_2 \xrightarrow[-PMe_3]{THF} \left[\begin{array}{c} Me_3P \\ Me_3P - Ni \\ Me_3P \end{array} \begin{array}{c} O \\ \| \\ C \\ O \end{array} \right] \xrightarrow[THF]{+PMe_3} Ni(PMe_3)_3(CO) + O=PMe_3$$

$$\qquad\qquad\qquad\qquad\qquad\qquad\qquad\qquad\quad \mathbf{4} \qquad\qquad\qquad\qquad \mathbf{5} \qquad\qquad \mathbf{6}$$

$$(6)$$

Surprisingly, treatment of CO_2 with a cold THF solution of $Ni(PMe_3)_4$ (Ni: $CO_2 = 1:1$) gave rise to nickel(0) complex $Ni(PMe_3)_3(CO)$ (**5**) in the yield of 32%, instead of the CO_2 adduct $(PMe_3)_3Ni(\eta^2\text{-}CO_2)$ (**4**) (Eq. (6)). Inspired by the unexpected result, we attempted to improve the yield of $(PMe_3)_3Ni(CO)$ (**4**) through raising the $Ni(PMe_3)_4$: CO_2 ratio. Unfortunately, even though the $Ni(PMe_3)_4$: CO_2 ratio was increased from 1:5 to 1:1, no appreciable change in the yield of $Ni(PMe_3)_3(CO)$ (**5**) was observed.

This result corresponds closely to that previously reported for $[(dtbpe)Ni]_2(\eta^2,\mu\text{-}C_6H_6)$ [19]. Therefore, we suggest that the $(PMe_3)_3Ni(\eta^2\text{-}CO_2)$ (**4**) is involved as an intermediate which is unstable and is likely to decompose under such conditions (Eq. (6)). Complex **5** exhibits infrared spectrum featuring a strong $\nu(CO)$ band at 1900 cm^{-1} that corresponds to that previously reported by Tolman [27]. It is proposed that the CO_2 ligand in **4** is reduced to CO with PMe₃ serving as reductant/O atom acceptor giving trimethylphosphine oxide, $O=PMe_3$, which was identified by ^1H and ^{31}P NMR. A similar reduction of CO_2 to CO at a nickel

center was observed for $[(dtbpe)Ni]_2(\eta^2,\mu\text{-}C_6H_6)$ [19] and $[MeC(CH_2PPh_2)_3]Ni(CO_2)$ [28], where a bidentate and tripodal phosphine served as an oxygen acceptor, respectively.

2.6. Comparison between molecular structures of **1** and **3**

By examining the structures complexes **1** and **3**, we could detect some geometrical difference between **1** and **3**. Complex **1** crystallizes in $P2_1/n$ space group, while compound **3** in Pbca space group. As seen in Figs. 1b and 2b, one of the phosphorus atoms, Pl, is contained in the plane defined by the Ni, C, and S atoms, which also is the mirror plane for the skeleton of the complexes. In both structures the angles P1–Ni1–P2 (104.17(4)⁰ (**1**); 103.29(3)⁰ (**3**)) and P1–Ni1–P3 (103.83(4)⁰ (**1**); 104.80(3)⁰ (**3**)) are smaller than 109.5⁰ for tetrahedral geometry (sp³ orbital hybridization), while P2–Ni1–P3 (116.94(4)⁰ (**1**); 120.49(3)⁰ (**3**)) are larger than 109.5⁰ because the influence of the coordinated CS_2 and PhNCS ligand. The greater deviation of angle P2–Ni1–P3 (120.49(3)⁰) in **3** from 109.5⁰ comparing with that of P2–Ni1–P3 (116.94(4)⁰ in **1** is caused by the larger molecular size of PhNCS comparing with that of CS_2. All of the Ni–P distances in both molecules are in the normal region.

We compare the geometries of compounds **1** and **3**. Here, the same P₃Ni fragment is interacted with two heteroallenic molecules that differ in the nature of the terminal groups, namely a sulfur atom in **1** and a NPh grouping in **3**. Some evident rearrangements have occurred in the geometry of the $P_3Ni(\eta^2\text{-}CS)$ fragment in the structure of **3**. The symmetry of the P₃Ni fragment in **1** and **3** belongs to C_s group. Moreover, the plane defined by the Ni, C, and S atoms contains P1 atom in these two compounds. The three Ni–P bonds are more asymmetrical in **3** since their lengths are different from each other: Ni1–P2 = 2.1870(7), Ni1–P1 = 2.1886(8) and Ni1–P3 = 2.2119(7) Å. Quite significant for the study of the interactions

between the metal fragment and the heteroallenic molecule is the lengthening of the Ni–S distance of about 0.03 Å on going from **1** to **3**. This is a clear indication of a weakened bond. In addition, the Ni–C distance is almost unchanged.

Other structural differences that emerge from the comparison of the two structures are as follows: (i) The C–S (coordinated) bond lengths are 1.647(3) and 1.707(2) Å in **1** and **3**, respectively. (ii) The bending of the coordinated η^2-CS_2 (S1–C1–S2 = 136.9(2)^0) in **1** is smaller than that of PhNCS (S1–C1–N1 = 142.23(16)^0) in **3** (Table 1). (iii) In both cases, the coordination to the metal affects both linkages that the carbon atom forms with the adjacent atom in CS_2 and SCNPh molecules. In fact, these linkages are shorter in the linear free (uncoordinated) molecules C–S = 1.55 Å in CS_2 [29]; C–S = 1.578 Å, C–N = 1.205 Å in SCNR (R = p-bromophenyl) [30]. This bond lengthening can be regarded as the bond activation (more precisely, weakened) by coordination. (iv) In compound **3** the phenyl ring attached to the nitrogen atom is not coplanar with the SCN plane, therefore, there is no symmetric plane in **3**.

2.7. Catalytic coupling reactions of organozinc with CS_2 catalyzed by **1**

Recently, Dong and coworkers reported nickel-catalyzed aryl- and alkylzinc carboxylations [16]. Complex **1** in our experiment has an approximately similar structure to that of Aresta's complex, $Ni(\eta^2$-$CO_2)(PCy_3)_2$ [12]. We were curious to know whether the nickel complex reported here would catalyze similar reactions. To the best of our knowledge, no method has been developed in metal-catalyzed organozinc coupling with CS_2. Herein, we attempted to use nickel complex **1** as the catalyst for coupling of organozinc with CS_2.

In our case, we found that in the presence of 10 mol% of **1** the coupling of dimethylzinc with CS_2 in THF at 40 °C followed by treatment with MeI due to the difficulties in isolation and characterization of dithiocarboxylic acids (Eq. 7), produced quantitatively methyl dithioacetate within 16 h (Table 2, entry 3). For complexes with different nickel sources, the catalysts showed distinct catalytic activity (Table 2, entries 4–6). Compared to **1**, other nickel complexes proved to be less reactive catalysts. To confirm that the reactions were catalyzed by nickel, control experiments were performed, and there were no significant coupling products observed (Table 2, entries 1 and 2).

To further extend the utility of our nickel catalysts, we explored the catalytic coupling of organozinc bearing different functionalities with CS_2 (Eq. 8). With 10 mol% of **1** as the catalyst, MeZnMe, EtZnEt and PhZnBr (Table 3, entries 1–3) coupled with CS_2 to form

Table 2
Catalytic coupling of dimethylzinc with CS_2.[a]

$$ZnMe_2 + CS_2 \xrightarrow[\text{(2) MeI, 50 °C, 3h}]{\text{(1) 10 mol\% [Ni], THF, 40 °C}} MeC(=S)SMe \quad (7)$$
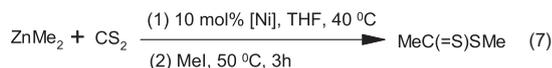
Entry	[Ni]	Ligand[b]	Time (h)	Yield (%)[c]
1	None	None	48	0
2	None	PMe_3	48	0
3	$(PMe_3)_3Ni(\eta^2$-$CS_2)$		16	42
4	$(PMe_3)_3Ni(\eta^2$-$CS_2)$	PMe_3	12	52
5	$Ni(COD)_2$	PMe_3	25	34
6	$NiCl_2$	PMe_3	65	16

[a] Reaction conditions: MeZnMe (2.2 mmol), CS_2 (2.0 mmol), and nickel complex **1** (10 mol%) in 2.0 mL of THF at 40 °C.
[b] With 20 mol% of PMe_3.
[c] GC-yield relative to CS_2 against internal standard (n-dodecane).

Table 3
Catalytic coupling of organozinc with CS_2.[a]

$$RZnX + CS_2 \xrightarrow[\text{(2) MeI, 50 °C, 3h}]{\text{(1) 10 mol\% [Ni], THF, 40 °C}} RC(=S)SMe \quad (8)$$
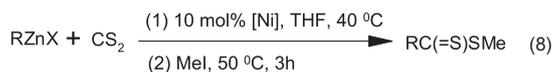
Entry	RZnX[b]	Time (h)	Yield (%)[c]
1	MeZnMe	16	52
2	EtZnEt	24	32
3	PhZnBr	12	64

[a] With 10 mol% of **1**, 20 mol% of PMe_3.
[b] Organozinc solution in THF.
[c] Isolated yields.

the corresponding methyl dithiocarboxylate following esterfication of the initial products.

3. Conclusions

In conclusion, the reactivity of $Ni(PMe_3)_4$ with CO_2, CS_2 and SCNPh has been studied. Although CO_2 is structurally homologous compound with CS_2 and SCNPh, its reactivity with $Ni(PMe_3)_4$ shows a different result with those of CS_2 and SCNPh. When CS_2 and SCNPh reacted with $Ni(PMe_3)_4$, complexes $(PMe_3)_3Ni(\eta^2$-$SCS)$ (**1**) and $(PMe_3)_3Ni(\eta^2$-$SCNPh)$ (**3**) were formed. Nickel(0) complexes **1** and **3** are stabilized by the strong donor ligand PMe_3. In the case of CO_2, attempts to isolate the expected nickel(0) complex $(PMe_3)_3Ni(\eta^2$-$CO_2)$ (**4**) proved to be unsuccessful. The CO_2 complex **4** was thermally unstable with respect to C–O bond cleavage and formed $(PMe_3)_3Ni(CO)$ (**5**) and O=PMe_3 (**6**). The reduction of CO_2 to CO is interesting, and other possible reductants (O-atom acceptors) have not been found to effect this transformation. Attempts to use $(PMe_3)_3Ni(\eta^2$-$SCS)$ (**1**) as catalyst for coupling reactions of organozinc and CS_2 were successful. In view of the outstanding performance of $Ni(PMe_3)_4$ in the activation or cleavage of C–S and C–O bond of CS_2, SCNPh and CO_2, we now plan to extend this work with the aim of producing more diverse applications for this novel system.

4. Experimental

4.1. General experimental methods

All reactions were carried out under nitrogen or argon atmosphere using standard vacuum-line techniques. Solvents were purified by standard procedures and were freshly distilled prior to use. Literature method was used in the preparation of tetrakis(trimethylphosphine)nickel(0) [31], Infrared spectra (4000–400 cm^{-1}), as obtained from Nujol mulls between KBr disks, were recorded on a Bruker alpha FT-IR. Melting points were recorded in capillary tubes. ^{1}H (300 MHz), ^{13}C (100.56 MHz) NMR spectra were recorded on a Bruker Avance 300 MHz spectrometer at room temperature. Chemical shifts cited were referenced to TMS (^{1}H, ^{13}C) as internal standard. Elemental analyses were carried out on an Elementar Vario EL III. X-ray crystallography was performed with a Bruker Smart 1000 diffractometer.

4.2. Synthesis of compound **1**

In a 100 mL round bottomed flask, CS_2 (314 mg, 4.14 mmol) in 30 mL of diethyl ether was combined with $Ni(PMe_3)_4$ (500 mg, 1.38 mmol) in 30 mL of diethyl ether at 0 °C. The reaction mixture

changed immediately from light yellow to red and was kept at room temperature for 24 h. During this period, some red powder precipitated from the diethyl ether solution. After filtration, the solvents were reduced to give a red solid, which crystallized from diethyl ether at $-20\,°C$. Yield: 405 mg, 81%; m.p. (dec) >120 °C. *Anal.* Calc. for $C_{10}H_{27}NiP_3S_2$ (363.06 g/mol): C, 33.04; H, 7.44; S, 17.63. Found: C, 33.01; H, 7.48; S, 17.58%. IR (Nujol, cm^{-1}): $\nu(C{=}S)$, 1149 vs.; $\nu(C–S)$, 638 vs. ^{1}H NMR (300 MHz, C_6D_6, 294 K, ppm): δ 1.05 (d, $^2J(PH) = 4.2$ Hz, PCH_3). ^{13}C NMR (75.5 MHz, C_6D_6, 294 K, ppm): δ 65.6 (s, CS_2), 127.8 (s, PCH_3). ^{31}P NMR (121.5 MHz, C_6D_6, 294 K): δ −28.3 (s, PCH_3).

4.3. Synthesis of compound 3

In a 100 mL round bottomed flask, SCNPh (559 mg, 4.14 mmol) in 30 mL of diethyl ether was combined with $Ni(PMe_3)_4$ (500 mg, 1.38 mmol) in 30 mL of diethyl ether at 0 °C. The reaction mixture changed immediately from light yellow to red and was kept at room temperature for 24 h. During this period, some red powder precipitated from the diethyl ether solution. After filtration, the solvents were reduced to give a red solid, which crystallized from diethyl ether at $-20\,°C$. Yield: 419 mg, 72%; m.p. (dec) >115 °C. *Anal.* Calc. for $C_{16}H_{32}NNiP_3S$ (422.11 g/mol): C, 45.4; H, 7.58; N, 3.31; S, 7.58. Found: C, 45.3; H, 7.62; N, 3.28; S, 7.60%. IR (Nujol, cm^{-1}): $\nu(C{=}N)$, 1607 s; $\nu(C–S)$, 656 vs. ^{1}H NMR (300 MHz, C_6D_6, 294 K, ppm): δ 1.01 (d, $^2J(PH) = 4.4$ Hz, PCH_3); δ 7.01–7.94 (m, 5H, aromatic-H). ^{13}C NMR (75.5 MHz, C_6D_6, 294 K, ppm): ^{13}C NMR (75.5 MHz, C_6D_6, 294 K, ppm): δ 65.6 (s, CS_2), 127.8 (s, PCH_3). ^{31}P NMR (121.5 MHz, C_6D_6, 294 K): δ −21.5 (s, PCH_3).

4.4. Reaction of $Ni(PMe_3)_4$ with CO_2

A 100 mL round bottomed flask was charged with a 40 mL diethyl ether solution of $Ni(PMe_3)_4$ (500 mg, 1.38 mmol). Gaseous carbon dioxide (60.72 mg, 1.38 mmol) was transferred into the THF solution of $Ni(PMe_3)_4$ in liquid nitrogen trap. The solution was stirred for 2 h at $-78\,°C$ before being gradually warmed to ambient temperature. During this time, the color of the solution changed gradually from light yellow to orange and white precipitate was also noted. After filtration, $Ni(PMe_3)_3(CO)$ (5) and $O{=}PMe_3$ (6) were obtained as indicated by ^{31}P NMR and by comparison to the IR spectra with those in the literature [23]. The yields of $Ni(PMe_3)_3(CO)$ (32%) and $O{=}PMe_3$ (39%) were determined by ^{31}P NMR.

4.5. X-ray crystallography

Intensity data were collected on a Bruker SMART diffractometer with graphite-monochromated Mo Kα radiation ($\lambda = 0.71073$ Å). Crystallographic data for complexes 1 and 3 are summarized in Table 4. The structures were solved by direct methods and refined with fullmatrix least-squares on all F^2 (SHELXL-97) with non-hydrogen atoms anisotropic.

CCDC 850128 and 850129 contain the supplementary crystallographic data for 1 and 3. These data can be obtained free of charge from The Cambridge Crystallographic Data Center via www.ccdc.cam.ac.uk/data_request/cif.

4.6. Representative procedure for the Ni-catalyzed organozinc coupling with CS_2

Under N_2 atmosphere, to a 25 mL Schlenk tube containing a solution of 1 (72.6 mg, 0.2 mmol) in 2 mL of THF were added an organozinc (2.2 mmol) and CS_2 (152 mg, 2.0 mmol). The reaction mixture was stirred at 40 °C until there was no CS_2 left (monitored by GC–MS). Then MeI was added to the mixture (1 mL). After the

Table 4
Crystallographic data for complexes 1 and 3.

Compound	1	3
Empirical formula	$C_{10}H_{27}NiP_3S_2$	$C_{16}H_{32}NNiP_3S$
Formula weight	363.06	422.11
Cryst syst	Monoclinic	Orthorhombic
Space group	$P2_1/n$	$Pbca$
Unit cell dimensions		
a (Å)	9.8240(16)	12.818(3)
b (Å)	15.124(3)	16.936(3)
c (Å)	13.127(2)	20.906(4)
β (°)	105.981(2)	90
V (Å^3)	1875.1(5)	4538.3(16)
Z	4	8
Θ_{max} (°)	26.53	28.40
D_{calc} (g cm^{-3})	1.286	1.236
μ (mm^{-1})	1.492	1.156
Crystal color	Dark red	Red
No. of reflections collected	20883	37941
No. of unique data	3893	5666
R_{int}	0.1339	0.0383
R_1 ($I > 2\sigma(I)$)	0.0353	0.0329
wR_2 indices (all data)	0.0657	0.0906

mixture was stirred for 3 h at 50 °C, the reaction was quenched by the slow addition of water (2 mL), and the organic phase was separated. The aqueous phase was extracted with pentane (2 × 1 mL); the combined organic phases were washed copiously with water (2 × 1 mL) to remove the tetrahydrofuran and dried with magnesium sulfate overnight. Distillation of the pentane through a short Vigreaux left an orange residue, which was further purified using flash column chromatography to give corresponding methyl dithiocarboxylate (eluted with 5 × 15% ethyl acetate in hexanes). The isolated sample was characterized by ^{1}H NMR analysis. ^{1}H NMR (300 MHz, $CDCl_3$, 294 K, ppm): methyl dithioacetate, $CH_3C(=S)SCH_3$, δ 2.62 (s, 3H), 2.86 (s, 3H) [32]; methyl dithiopropionate, $CH_3CH_2C(=S)SCH_3$, δ 0.98 (t, 3H), 2.90 (s, 3H), 1.72 (q, 2H); methyl dithiobenzoate, $C_6H_5C(=S)SCH_3$, δ 2.82 (s, 3H), 7.36–7.51 (m, 5H).

Acknowledgments

References

[1] K.K. Pandey, Coord. Chem. Rev. 140 (1995) 37.
[2] J.A. Ibers, Chem. Soc. Rev. 11 (1982) 57.
[3] H. Werner, Coord. Chem. Rev. 43 (1982) 165.
[4] M. Aresta, A. Dibenedetto, Dalton Trans. (2007) 2975.
[5] T. Sakakura, J.-C. Choi, H. Yasuda, Chem. Rev. 107 (2007) 2365.
[6] J. Louie, Curr. Org. Chem. 9 (2005) 605.
[7] H. Arakawa, M. Aresta, J.N. Armor, M.A. Barteau, E.J. Beckman, A.T. Bell, J.E. Bercaw, C. Creutz, E. Dinjus, D.A. Dixon, K. Domen, D.L. DuBois, J. Eckert, E. Fujita, D.H. Gibson, W.A. Goddard, D.W. Goodman, J. Keller, G.J. Kubas, H.H. Kung, J.E. Lyons, L.E. Manzer, T.J. Marks, K. Morokuma, K.M. Nicholas, R. Periana, L. Que, J. Rostrup-Nielson, W.M.H. Sachtler, L.D. Schmidt, A. Sen, G.A. Somorjai, P.C. Stair, B.R. Stults, W. Tumas, Chem. Rev. 101 (2001) 953.
[8] L.D. Field, E.T. Lawrenz, W.J. Shaw, P. Turner, Inorg. Chem. 39 (2000) 5632.
[9] A. Del Zotto, E. Rocchini, F. Pichierri, E. Zangrando, P. Rigo, Inorg. Chim. Acta 299 (2000) 180.
[10] A.S. Batsanov, A.V. Churakov, J.A.K. Howard, A.K. Hughes, A.L. Johnson, A.J. Kingsley, I.S. Neretin, K. Wade, J. Chem. Soc., Dalton Trans. 21 (1999) 3867.
[11] J. Vicente, M.T. Chicote, P. González-Herrero, P.G. Jones, Chem. Commun. 21 (1997) 2047.
[12] M. Aresta, C.F. Nobile, V.G. Albano, E. Forni, M. Manassero, J. Chem. Soc., Chem. Commun. 15 (1975) 636.
[13] M. Aresta, C.F. Nobile, J. Chem. Soc., Dalton Trans. 7 (1977) 708.
[14] M. Aresta, R. Gobetto, E. Quaranta, I. Tommasi, Inorg. Chem. 31 (1992) 4286.
[15] C.H. Lee, D.S. Laitar, P. Mueller, J.P. Sadighi, J. Am. Chem. Soc. 129 (2007) 13802.
[16] C.S. Yeung, V.M. Dong, J. Am. Chem. Soc. 130 (2008) 7826.
[17] M.A. Bennett, J.A. Johnson, A.C. Willis, Organometallics 15 (1996) 68.

[18] T. Yamamoto, T. Kohara, K. Osakada, A. Yamamoto, Bull. Chem. Soc. Jpn. 56 (1983) 2147.
[19] J.S. Anderson, Inorg. Chem. 49 (2010) 10203.
[20] H.F. Klein, H.H. Karsch, Chem. Ber. 109 (1976) 2515.
[21] H. Werner, Coord. Chem. Rev. 43 (1982).
[22] R.O. Harris, J. Powell, A. Walker, P.V. Yaneff, J. Organomet. Chem. 141 (1977) 217.
[23] C. Bianchini, D. Masi, C. Mealli, A. Meli, J. Organomet. Chem. 247 (1983) C29.
[24] C. Bianchini, D. Masi, C. Mealli, A. Meli, Inorg. Chem. 23 (1984) 2838.
[25] S. Gambarotta, M.L. Fiallo, C. Floriani, A. Chiesi-Villa, C. Guastini, Inorg. Chem. 23 (1984) 3532.
[26] R. Flugel, O. Gevert, H. Werner, Chem. Ber. 129 (1996) 405.
[27] C.A. Tolman, J. Am. Chem. Soc. 92 (1970) 2956.
[28] C. Bianchini, D. Masi, C. Mealli, A. Meli, M. Sabat, Inorg. Chem. 23 (1984) 2731.
[29] A.H. Guenter, J. Chem. Phys. 31 (1959) 1095.
[30] L. Ulicky, Zb. Pr. Chemickotechnol. Fak. SVST 47 (1969) 288.
[31] H.-F. Klein, H.H. Karsch, Angew. Chem. 82 (1970) 885.
[32] F.L. Lu, J. Org. Chem. 54 (1989) 2165.